Polyethylene Glycol Coated NiFe$_2$O$_4$ Nanoparticles Produced by Solution Plasma Method for Biomedical Applications

Masoud Shabani, Ehsan Saebnoori[*], Seyed Ali Hassanzadeh-Tabrizi, Hamid Reza Bakhsheshi-Rad

Advanced Materials Research Center, Department of Materials Engineering, Najafabad Branch, Islamic Azad University, Najafabad, Iran.

ARTICLE INFO

ABSTRACT

The structural and magnetic properties of the polyethylene glycol (PEG) coated nickel spinel ferrite (NiFe$_2$O$_4$) nanoparticles have been reported in the present study. NiFe$_2$O$_4$ nanoparticles were prepared by solution plasma method using KOH + Na$_2$Co$_3$ as electrolyte. The prepared powder of nickel ferrite nanoparticles was annealed at 800 ˚C for two h and used for further study. The X-ray analysis confirmed the formation of a cubic spinel single-phase structure. The crystallite size, lattice parameter, and X-ray density of the PEG-coated NiFe$_2$O$_4$ nanoparticles were calculated using XRD data. TEM and FTIR studies revealed the presence of PEG on nickel ferrite nanoparticles and reduced agglomeration in the NiFe$_2$O$_4$ nanoparticles. The pulse-field hysteresis loop tracer technique studied the magnetic properties at room temperature. The magnetic parameters such as saturation magnetization, remanence magnetization, and coercivity have been obtained. These magnetic parameters were get decreased by PEG coating.

[*] **Corresponding Author:**
Email Address: ehsan.saebnoori@gmail.com

1. Introduction

In recent years, spinel ferrite nanoparticles have been the subject of advanced research. The spinel ferrite has a structural formula MFe_2O_4, where M is a divalent metal with a cubic spinel crystal structure. In addition, the spinel ferrite has magnetic properties. Magnetic nanoparticles can be used in various applications such as adsorbents [1, 2], magnetic storage, ferrofluids, biomedical applications [3, 4], and gas sensors [5]. Nickel ferrite ($NiFe_2O_4$) is one of the widely used spinel ferrites in various biomedical applications. It has an inverse spinel structure showing ferromagnetism that originates from the magnetic moment of anti-parallel spins between Fe^{3+} ions at tetrahedral sites and Ni^{2+} ions at octahedral sites [6]. By now, various methods such as the combustion method [7], organic gel-thermal decomposition method [8], sol-gel auto combustion method [9], and co-precipitation method [10] have been developed to prepare nano crystallite nickel ferrite. However, each of these methods has limitations. Recently, the in-liquid plasma or solution plasma has been employed to synthesize nanoparticles [11, 12]. This method has advantages over other methods such as inexpensive raw materials, simple equipment, no need for a vacuum chamber, no gas supply requirement, easy separation of products from solution, alternating current (AC), and high purity [13]. Several natural and synthetic polymers have been employed to modify the surface of the magnetic nanoparticles. These polymers include starch, dextran, polyvinyl alcohol, lauric acid, dendrimers, polyethylene glycol, chitosan, oleic acid. Polyethylene glycol (PEG) is a polymer consists of ethylene oxide and water. PEG is water-soluble, inert in biological systems, non-toxic, does not influence cell viability, hydrophilic material for biomedical applications. The structural and magnetic properties of the $NiFe_2O_4$ produced by the solution plasma method and polyethylene glycol (PEG) coated $NiFe_2O_4$ nanoparticles have been reported in the present study. Nickel ferrite nanoparticles have not been produced by the solution plasma method so far, and by using the appropriate composition and concentration of electrolyte, the voltage required to produce nanoparticles has been reduced compared to other studies. Also, two metal elements have been used in the target electrode, and these two metal elements have entered the final composition of nanoparticles with oxygen.

2. Experimental

2.1. Materials and synthesis of $NiFe_2O_4$ nanoparticles

KOH and Na_2CO_3 (AR grade, Merck, 99%) were used as the precursors. Iron and nickel powders with a particle size of fewer than 70 micrometers were used to prepare the anode, and an AISI 316 stainless steel sheet (200 mm × 100 mm × 0.5 mm) was used as the cathode. The powders of iron and nickel were sintered at the temperature of 900 ˚C, the pressure of 40 Mpa, and holding times of 10 min in a Spark Plasma Sintering (SPS) chamber. By connecting to the AC power supply in the solution plasma process, the glow discharge plasma was generated around the anode, and the $NiFe_2O_4$ nanoparticles were synthesized [11]. The solution with a concentration of 3 molars (with a weight ratio of 1:1) was used for the synthesizing. The applied voltage is increased with a 1 V/min speed and then fixed at a constant value (23 V) for 100 min. The as-synthesized powder was annealed at 800 ˚C for two h in the air environment to remove the impurities [14]. Figure 1 shows the production steps of nickel ferrite nanoparticles by the solution plasma method.
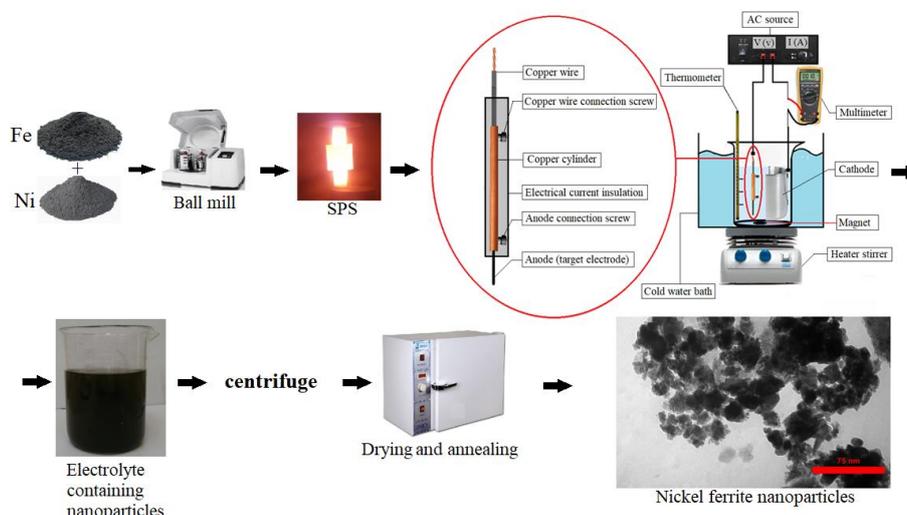

Fig. 1. The production process of nickel ferrite nanoparticles using the solution plasma method.

2.2. Coating of $NiFe_2O_4$ nanoparticles with Polyethylene glycol (PEG)

Nickel ferrite nanoparticles were coated with PEG-4000. The aqueous PEG solution (0.77 grams) was prepared by dissolving PEG in 24.48 ml distilled water and stirred for 30 minutes. Then 0.255 grams of $NiFe_2O_4$ nanoparticles were added and stirred for ten h at 45 ˚C for their dispersion. Further, it was allowed to sonicate for 20 min. Then, the mixture of nanoparticles and PEG was centrifuged for 10 min, washed three times using deionized water in an oven, and dried at 60 °C for 12 hours to remove excess PEG. The resulting nanoparticles were dried at room temperature to yield PEG-coated $NiFe_2O_4$ nanoparticles.

2.3. Characterization

The phase identification and crystallite size determination were made by XRD analysis with a Bruker D8 X-ray diffractometer equipped with a crystal monochromator employing Cu-Kα radiation of wavelength 1.5418 Å in 2θ range from 20 to 85. The Scherrer formula was used to obtain the average size of crystal D from the widening of the XRD peak line corresponding to all planes of spine structure [15, 16]. The magnetic characterization was carried out by vibrating sample magnetometer (VSM, Meghnatis Daghigh Kavir Co, Iran) under the applied magnetic field of ±15000 (Oe) at room temperature. The saturation magnetization (Ms), remanence magnetization (Mr), and coercivity (Hc) were determined from the observed M-H plots. The uncoated and coated sample morphology was studied by transmission electron microscope (TEM, Philips, CM120, Netherland). The surfactant coating was investigated using an FTIR spectroscope (AVATAR, Thermo, USA) using KBr pellets in the range of 400-4000 cm^{-1} with a resolution of 4 cm^{-1}.

3. Results and discussion

The X-ray diffraction patterns of the $NiFe_2O_4$ nanoparticles have impurities before annealing (NP), annealed nickel ferrite nanoparticles (NP800), and PEG-coated $NiFe_2O_4$ nanoparticles (NP800-PEG) are shown in Figure 2. It indicates that the nanoparticles prepared before annealing consist of $NiFe_2O_4$, NiO, and α-Fe_2O_3. The product after annealing is a single phase and has a cubic spinel structure following JCPDS file No.01-86-2267. The main peak of $NiFe_2O_4$ that appears on 2θ corresponds to the reflection planes (220), (311), (222), (400), (331), (422), (511), (620), (533), (622) and (444). Moreover, it can be seen from Figure 2 that the diffraction peaks are weaker in intensity and broader for the $NiFe_2O_4$ nanoparticles obtained at higher addition of PEG. It indicates that the crystallinity decreases for the modified PEG-coated nanoparticles. The sharpening of the peaks (NP800-PEG) is due to the increase in the size after PEG coating. The structural parameters include crystallite size, lattice parameter, X-ray density using the Scherrer equation (Eq. 1) for the most substantial peaks (311), (400), and (440) of NP, NP800, and NP800-PEG were obtained given in Table 1.

$$D = \frac{K\lambda}{\beta \cos\theta} \tag{1}$$

where K is the Scherrer constant, β is the full-width half maximum (FWHM) of the diffraction peak, θ is the Bragg's angle, and λ is the wavelength of Cu-Kα = 1.5406 Å.
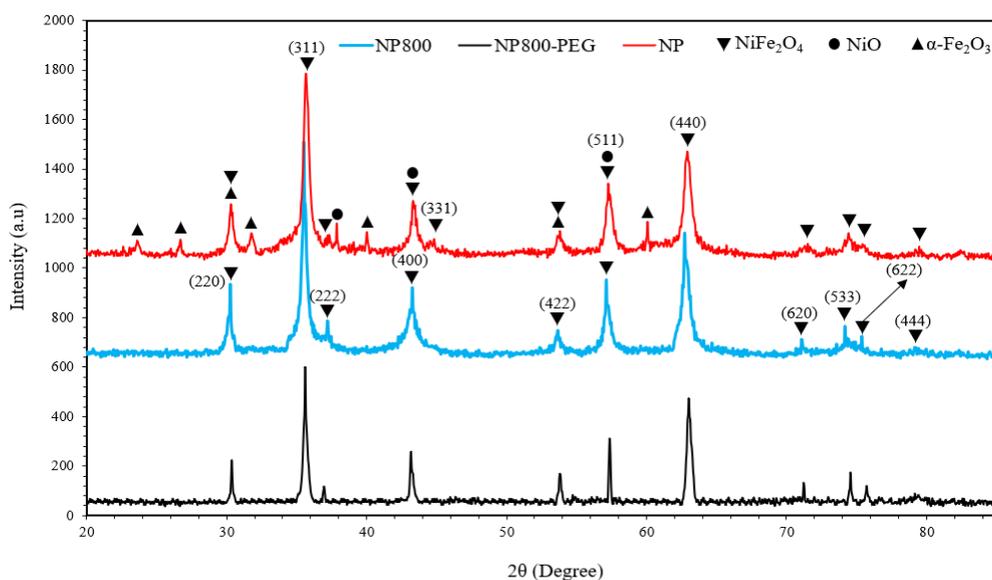

Fig. 2. X-ray diffraction patterns of $NiFe_2O_4$ nanoparticles before annealing (NP), annealed $NiFe_2O_4$ nanoparticles (NP800), and PEG-coated $NiFe_2O_4$ nanoparticles (NP800-PEG).

Table 1. Calculation of crystallite size based on FWHM by using the Scherer equation.

Sample	2θ (311) (Deg.)	2θ (400) (Deg.)	2θ (440) (Deg.)	Inter planar spacing (Å)	Lattice parameter (Å)	β (311) (Rad)	β (400) (Rad)	β (440) (Rad)	D average (nm)
NP	35.57	43.65	62.76	2.5110	8.338	0.0066	0.0158	0.0137	15
NP800	35.46	43.46	62.69	2.5100	8.340	0.0045	0.0183	0.0141	19
NP800-PEG	35.51	43.33	62.64	2.5121	8.333	0.0037	0.0106	0.0118	24

The similar diffraction patterns of PEG-coated $NiFe_2O_4$ nanoparticles with that of $NiFe_2O_4$ nanoparticles suggest that the crystalline structure of $NiFe_2O_4$ nanoparticles did not change on the modification of the particles by PEG coating. It indicates that the PEG coating occurs only at the surface of $NiFe_2O_4$ nanoparticles. According to Table 1, the calculated value of the lattice parameter of $NiFe_2O_4$ nanoparticles after annealing is 8.340 Å which agrees with the reported matter, while that of PEG-coated $NiFe_2O_4$ nanoparticles is 8.333 Å [17].

The crystallite size of the NP800 nanoparticles is 32 nm, and that of PEG-coated $NiFe_2O_4$ nanoparticles is 40 nm.

Figure 3 (a and b) shows the surface morphology of pure $NiFe_2O_4$ nanoparticles after annealing (NP800) and PEG-coated $NiFe_2O_4$ nanoparticles (NP800-PEG). TEM images show that uncoated $NiFe_2O_4$ nanoparticles are highly agglomerated, while PEG-coated $NiFe_2O_4$ nanoparticles show a well-dispersed structure with few agglomerates. It may be due to the coating of PEG on nanoparticles.
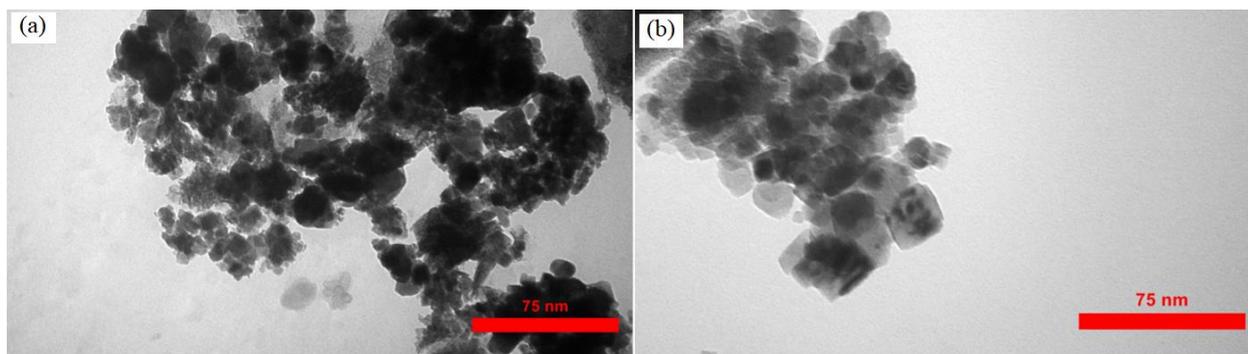

Fig. 3. TEM images of (a) NP800 and (b) NP800-PEG.

Figure 4 shows FTIR spectra of NP800, NP800-PEG, and pure PEG. From figure 4, the observed bonds under 1000 cm^{-1} are attributed to the metal oxide vibration (M↔O) bonds. The two prominent metal-oxygen bands at 400-630 cm^{-1} are seen in the FT-IR spectrum of the synthesized nickel ferrite sample. In crystal lattices, these two bands are usually assigned to the vibration of ions [18]. These bonds confirm the formation of the $NiFe_2O_4$ phase, and the vibrations of M↔O bonds at tetrahedral and octahedral sites are assigned to these peaks and indicate uniformly distributed ferrite particles [19].

Also, it observed that in the sample coated with polyethylene glycol, the two peaks related to the formation of nickel ferrite had moved slightly to the right compared to the uncoated nanoparticles. According to studies, the transfer of these two peaks to the right and their shortness in the coated nanoparticles is due to polyethylene glycol in the nanoparticles [2]. The intensive peak observed at about 3450 cm^{-1} and the less intensive peak at about

1650 cm^{-1} in curves (PEG, NP800, and NP800-PEG) occurred due to stretching vibration between hydrogen and oxygen atoms [6, 20]. In the NP800-PEG turn, the bands at about 2900 cm^{-1} represent the characteristic bond of the CH_2 group, as present in PEG. According to studies, the transfer of these two peaks to the right and their shortness in the coated nanoparticles is due to polyethylene glycol in the composition of the nanoparticles [2]. Thus, it reveals that the coating of PEG on the surface of $NiFe_2O_4$ nanoparticles has been successfully achieved. Figure 5 shows the magnetic results of the $NiFe_2O_4$ nanoparticles have impurities before annealing (NP), nanoparticles after annealing (NP800), and NP800-PEG in the range of ±15000Oe. It reveals that NP800 has high saturation magnetization than NP800-PEG. However, due to impurities, a weaker magnetic property was obtained in the NP sample. The nanoparticles before annealing have impurities α-Fe_2O_3 and NiO. These impurities can interfere with the magnetic moment's interaction and thus reduce

the structure's magnetic properties [2, 21]. The decrease in saturation magnetization in the NP800-PEG compared to NP800 is the formation of a polymer coating on nanoparticles because polyethylene glycol has a diamagnetic behavior that decreases saturation magnetization [22]. Magnetic properties (M_s, M_r, and H_c) are strongly dependent on

the crystallinity of nanoparticles possessing a large surface-to-volume ratio, and disorders reduce the magnetic properties of the synthesized nanoparticles [23]. The graph indicates a decrease in M_s of PEG-coated magnetic nanoparticles with a saturation magnetization (M_s) value of 42.52 emu/g over the NP800 with the value of 51.28 emu/g.
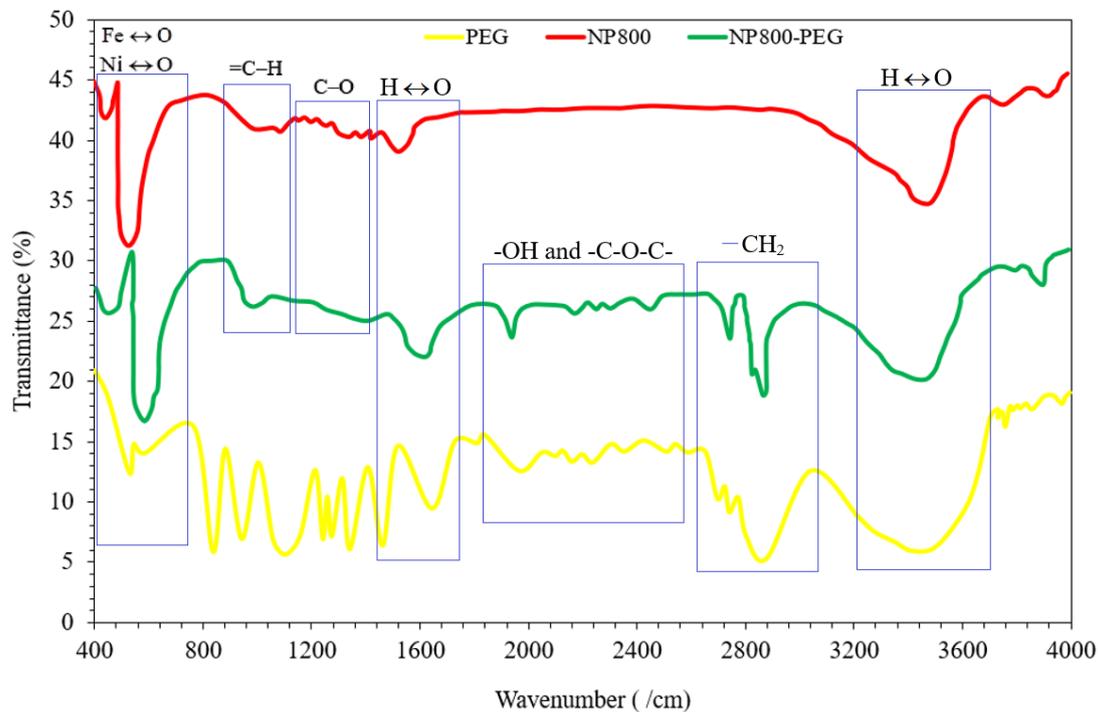

Fig. 4. FTIR spectra of pure $NiFe_2O_4$ nanoparticles (NP800), PEG-coated $NiFe_2O_4$ nanoparticles (NP800-PEG), and pure PEG.
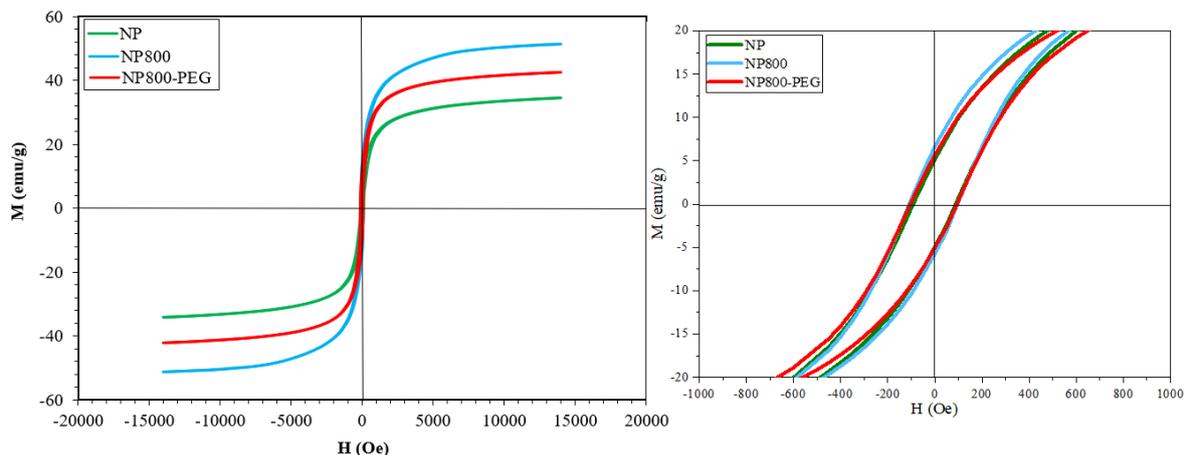

Fig. 5. VSM-Magnetic hysteresis of NP, NP800, and PEG-coated $NiFe_2O_4$ nanoparticles.

4. Conclusion

$NiFe_2O_4$ magnetic nanoparticles were synthesized using the solution plasma method and coated with polyethylene glycol (PEG). The XRD analysis confirms the phase formation with average crystalline sizes of 22, 32, and 40 nm of bare and PEG-coated magnetic nanoparticles. The FTIR analysis of barely coated nanoparticles confirms

surface modification with PEG with its prominent peak observed in the spectrum. The VSM analysis signifies PEG-coated nanoparticles have low saturation magnetization than bare nanoparticles. The encapsulation of PEG gets down the magnetic properties of nanoparticles, which results in a decrease in saturation magnetization from 51.28 to 42.52 (emu/g).

References

[1] Y. Sharma, V. Srivastava, Comparative studies of removal of Cr (VI) and Ni (II) from aqueous solutions by magnetic nanoparticles, Journal of Chemical & Engineering Data 56(4) (2011) 819-825.

[2] P.L. Hariani, D. Desnelli, F. Fatma, I.P. Rizki, S. Salni, Synthesis and characterization of Fe3O4 nanoparticles modified with polyethylene glycol as antibacterial material, The Journal of Pure and Applied Chemistry Research 7(2) (2018) 122.

[3] S. Sam, A.S. Nesaraj, Preparation of MnFe2O4 nanoceramic particles by soft chemical routes, Int J Appl Sci Eng 9(4) (2011) 223-239.

[4] Y. Prabhu, K.V. Rao, B.S. Kumari, V.S.S. Kumar, T. Pavani, Synthesis of Fe 3 O 4 nanoparticles and its antibacterial application, International Nano Letters 5(2) (2015) 85-92.

[5] R.H. Vignesh, K.V. Sankar, S. Amaresh, Y.S. Lee, R.K. Selvan, Synthesis and characterization of MnFe2O4 nanoparticles for impedometric ammonia gas sensor, Sensors and Actuators B: Chemical 220 (2015) 50-58.

[6] S. Maensiri, C. Masingboon, B. Boonchom, S. Seraphin, A simple route to synthesize nickel ferrite (NiFe2O4) nanoparticles using egg white, Scripta materialia 56(9) (2007) 797-800.

[7] J. Zhu, D. Xiao, J. Li, X. Yang, Y. Wu, Characterization of FeNi3 alloy in Fe–Ni–O system synthesized by citric acid combustion method, Scripta materialia 54(1) (2006) 109-113.

[8] L. Guo, X. Shen, X. Meng, Y. Feng, Effect of Sm3+ ions doping on structure and magnetic properties of nanocrystalline NiFe2O4 fibers, Journal of Alloys and Compounds 490(1-2) (2010) 301-306.

[9] S.M. Peymani-Motlagh, A. Sobhani-Nasab, M. Rostami, H. Sobati, M. Eghbali-Arani, M. Fasihi-Ramandi, M.R. Ganjali, M. Rahimi-Nasrabadi, Assessing the magnetic, cytotoxic and photocatalytic influence of incorporating Yb 3+ or Pr 3+ ions in cobalt–nickel ferrite, Journal of Materials Science: Materials in Electronics 30(7) (2019) 6902-6909.

[10] P. Sivakumar, R. Ramesh, A. Ramanand, S. Ponnusamy, C. Muthamizhchelvan, Preparation of sheet like polycrystalline NiFe2O4 nanostructure with PVA matrices and their properties, Materials Letters 65(9) (2011) 1438-1440.

[11] M. Shabani, E. Saebnoori, S. Hassanzadeh-tabrizi, H.R. Bakhsheshi-Rad, Novel synthesis of nickel ferrite magnetic nanoparticles by an in-liquid plasma, Journal of Materials Science: Materials in Electronics 32(8) (2021) 10424-10442.

[12] Y. Toriyabe, S. Watanabe, S. Yatsu, T. Shibayama, T. Mizuno, Controlled formation of metallic nanoballs during plasma electrolysis, Applied physics letters 91(4) (2007) 041501.

[13] S. Samimi-Sedeh, E. Saebnoori, A. Hassanzadeh, An optimization and characterization study on sodium ferrate production by electrochemical method, Journal of Advanced Materials and Processing 7(4) (2019) 3-11.

[14] M. Jalaly, M. Enayati, P. Kameli, F. Karimzadeh, Effect of composition on structural and magnetic properties of nanocrystalline ball milled Ni1− xZnxFe2O4 ferrite, Physica B: Condensed Matter 405(2) (2010) 507-512.

[15] L. Whittig, X-ray diffraction techniques for mineral identification and mineralogical composition, Methods of Soil Analysis: Part 1 Physical and Mineralogical Properties, Including Statistics of Measurement and Sampling 9 (1965) 671-698.

[16] K. Kombaiah, J.J. Vijaya, L.J. Kennedy, M. Bououdina, Studies on the microwave assisted and conventional combustion synthesis of Hibiscus rosa-sinensis plant extract based ZnFe2O4 nanoparticles and their optical and magnetic properties, Ceramics International 42(2) (2016) 2741-2749.

[17] S. Yadav, S. Shinde, A. Kadam, K. Rajpure, Structural, morphological, dielectric and magnetic properties of Mn substituted cobalt ferrite, Journal of Semiconductors 34(9) (2013) 093002.

[18] P.G. Rasmussen, Far-infrared and Raman spectra ofpseudo-tetrahedral complexes of ethylenedimorpholene, Transition Metal Chemistry 11(11) (1986) 416-418.

[19] Z. Zhou, J. Xue, J. Wang, H. Chan, T. Yu, Z. Shen, NiFe 2 O 4 nanoparticles formed in situ in silica matrix by mechanical activation, Journal of applied physics 91(9) (2002) 6015-6020.

[20] S. Saafan, T. Meaz, E. El-Ghazzawy, M. El Nimr, M. Ayad, M. Bakr, AC and DC conductivity of NiZn ferrite nanoparticles in wet and dry conditions, Journal of magnetism and Magnetic materials 322(16) (2010) 2369-2374.

[21] C.-S. Lin, C.-C. Hwang, T.-H. Huang, G.-P. Wang, C.-H. Peng, Fine powders of SrFe12O19 with SrTiO3 additive prepared via a quasi-dry combustion synthesis route, Materials Science and Engineering: B 139(1) (2007) 24-36.

[22] Z.E. Gahrouei, S. Labbaf, A. Kermanpur, Cobalt doped magnetite nanoparticles: Synthesis, characterization, optimization and suitability evaluations for magnetic hyperthermia applications, Physica E: Low-dimensional Systems and Nanostructures 116 (2020) 113759.

[23] M. Lickmichand, C.S. Shaji, N. Valarmathi, A.S. Benjamin, R.A. Kumar, S. Nayak, R. Saraswathy, S. Sumathi, N.A.N. Raj, In vitro biocompatibility and hyperthermia studies on synthesized cobalt ferrite nanoparticles encapsulated with polyethylene glycol for biomedical applications, Materials Today: Proceedings 15 (2019) 252-261.